Landsliding related to land-cover change: A diachronic analysis of hillslope instability distribution in the Sierra Norte, Puebla...

Article *in* Catena · February 2006

DOI: 10.1016/j.catena.2005.11.006

Irasema Alcántara-Ayala
Universidad Nacional Autónoma de México

Available online at www.sciencedirect.com
SCIENCE @ DIRECT®
Catena 65 (2006) 152 – 165
CATENA
www.elsevier.com/locate/catena

Landsliding related to land-cover change: A diachronic analysis of hillslope instability distribution in the Sierra Norte, Puebla, Mexico

I. Alcántara-Ayala *, O. Esteban-Chávez, J.F. Parrot

Institute of Geography, UNAM Circuito Exterior, Ciudad Universitaria, Coyoacán, 04510, Mexico, D.F.

Abstract

This study examines mass movement associated with land use change, particularly deforestation, from multiple perspectives. The significance of such understanding is related to the degree of impact landsliding may cause on human settlements and economic activities, and on forest ecosystems. In this paper, the distribution of hillslope instability in the Sierra Norte, Puebla, Mexico is addressed by means of a diachronic analysis, which involves the development of vegetation indexes, as well as vegetation fragmentation derived from Landsat-5 (TM) and Landsat-7 (ETM+) satellite images from 1989 and 1999, respectively. The time period was chosen to compare vegetation cover conditions prior and after the extreme October 1999 rainfall event that triggered hundreds of slope failures in the study area. Results suggested there was a significant vegetation reduction from 1989 to 1999, which was strongly expressed by an increase of 809 km^2 of bare surfaces. Additionally, areas with highest vegetation density (91 – 100%) decreased considerably, from 1245 to 363 km^2, resulting in a net vegetation reduction of 70%. Furthermore, it was possible to highlight that landslide concentration was much higher on surfaces that were bare and had low vegetation density (0 – 50%), representing 85% of hillslope instability, than on surfaces having a greater density of vegetation cover. Land use change and land degradation are precursors to environmental hazards, such as mass movement events, that pose serious threats to regional population distributions and economic vitality.

Keywords: Land-cover change; Mass movement; Land degradation; Satellite images; Sierra Norte Puebla, Mexico

1. Introduction

Mass movement are gravity driven events that occur naturally, but are also triggered by anthropogenic influence on the environment. Land use change drives land degradation, and can make hillslopes more susceptible to mass movement. The past several decades have been characterized by an intense disruption of natural vegetation. In combination with extreme meteorological events, this form of land use change is associated with a global increase in landslides, having a significant impact principally in developing or less developed countries. Such impact is derived from two main aspects (Alcántara-Ayala, 2002). First, least developed countries are located to a great extent in zones largely affected by natural hazards, for instance seismicity, volcanic activity, flooding and indeed mass movement. Secondly, the historical development of these countries involves high levels of vulnerability, which when coupled with natural forces, results in a cycle of disasters and environmental disturbance.

This study examines spatial relationships between vegetation cover and landsliding by a diachronic analysis of hillslope instability distribution in the Sierra Norte, Puebla, Mexico; a region greatly impacted by rainfall induced slope failures in October 1999. The analysis involves comparing vegetation cover scenarios using satellite images from 1989 and 1999 to examine land use and forest conditions prior and after the extreme rainfall event that triggered slope instability.

Over the 20th century landsliding resulted in more than 50,000 victims, affecting almost 10 million inhabitants, and involved economic losses of 3500 millions of US dollars (EM-DAT: OFDA/CRED Database). With the

* Corresponding author. Tel.: +52 55 56 22 43 39; fax: +52 55 56 16 21 45.
E-mail address: irasema@igiris.igeograf.unam.mx (I. Alcántara-Ayala).

0341-8162/$ - see front matter © 2005 Elsevier B.V. All rights reserved.
doi:10.1016/j.catena.2005.11.006

exception of Africa and Australia, and Antarctica, during this period, 1903 to 2003, the American, European, and Asian continents were greatly impacted by the loss of human lives due to landsliding. Concerning the total affected population, Asia has been impacted the most (Table 1), which is associated with very high levels of vulnerability. Disasters due to landsliding has produced severe losses and damage in places such as Tajikistan, China, Peru, Colombia, Central America, and Venezuela (Table 2).

In many instances landsliding is associated with deforestation, but it is important to note that cause–effect relationships may be reversed. Many mass movement are caused by areas that have undergone significant deforestation. However, landslides are also responsible for damage to forest ecosystems (Table 3). In any case, forest extent, condition, and productivity represent a crucial global concern, as argued by the World Bank (2002), with respect to the role of forest resources in the livelihoods of 90% of the 1.2 billion people living in conditions of extreme poverty. Indirectly forest resources are crucial to supporting the natural environment by nurturing agriculture and food supplies of nearly half the population of least developed countries. Indeed, there are approximately 60 million indigenous people entirely dependent on forests. Additionally, forest ecosystems comprise practically 90% of terrestrial biodiversity.

The influence of land use change on mass movement under different geomorphic conditions has been addressed by researchers taking into account different methods (Pande et al., 2002), including historical archives (Glade, 2003), aerial photographs interpretation (Su and Stohr, 2000), mapping, multivariate statistical analyses, laboratory and field investigations (Gerrard and Gardner, 2002), monitoring (Keppeler et al., 1994), modeling (Abe and Ziemer, 1991a,b; Ziemer, 1991; Wu and Thornes, 1996; Montgomery et al., 2000; Van Beek and Van Asch, 2004), geographical information systems (Temesgen et al., 2001), and remote sensing (De La Ville et al., 2002). In particular, remote sensing can be regarded as a useful tool to address landsliding studies at a local and regional scale, over several decades of time.

Table 2
Top 10 countries affected by landsliding (EM-DAT: OFDA/CRED Database)

Country	Date	Killed
Soviet Union	1949	12,000
Peru	December 1941	5000
Honduras	September 20, 1973	2800
Peru	January 10, 1962	2000
Italy	October 9, 1963	1189
India	October 1, 1968	1000
Colombia	September 27, 1987	640
Peru	March 18, 1971	600
China P Rep	March 23, 1934	500
India	September 18, 1948	500

Country	Date	Affected
Brazil	January 11, 1966	4,000,000
India	July 1986	2,500,000
India	September 12, 1995	1,100,000
Nepal	July 15, 2002	265,865
Indonesia	March 31, 2003	229,548
Philippines	December 19, 2003	217,988
India	August 17, 1998	200,000
Bolivia	February 1994	165,000
Brazil	August 2000	143,000
Chile	June 19, 1991	82,811

Local landslides analysis certainly implies a follow-up of the evolution of the process, while at a regional level, correlations among controlling factors are determined (Marston et al., 1998).

2. Research site

2.1. Landsliding in the Sierra Norte, Puebla

Puebla is located east of Mexico City (Fig. 1) and is situated at the transition of the Trans-Mexican Volcanic Belt and the Sierra Madre Oriental physiographic provinces. The former consists of a series of Late Tertiary and Quaternary volcanoes and associated landforms such as domes and calderas essentially of calc-alkaline type (Alva-Valdivia et al., 2000), and the latter is primarily comprised of Mesozoic sedimentary rocks. The Sierra Norte is located in the

Table 1
Population affected by landsliding in the world regions (EM-DAT: OFDA/CRED Database)

	No. of events	Killed	Injured	Homeless	Affected	Total affected	Damage US (000's)
Africa	22	721	56	7936	11,748	19,740	0
Average per event		33	3	361	534	897	0
America	137	20,492	4726	186,682	4,470,690	4,662,098	1,317,927
Average per event		150	35	1363	32,633	34,030	9620
Asia	215	15,639	3429	3,742,516	1,309,696	5,055,641	534,229
Average per event		73	16	17,407	6092	23,515	2485
Europe	75	16,158	743	3125	37,668	41,536	1,705,689
Average per event		215	10	42	502	554	22,743
Oceania	15	528	52	8000	2963	11,015	2466
Average per event		35	4	533	198	734	164

Table 3
Impact of landsliding on vegetation cover

Date	Location	Triggering mechanism	Impact	References
1935	Papua New Guinea (Torricelli Range)	Earthquake $M=7.9$	130 km^2 of vegetation removal	Marshall (1937), Simonett (1967), Garwood et al. (1979), Schuster and Highland (2003)
1960	Chile (Valdivian Andes)	Earthquake $M=9.2$	More than 250 km^2 of temperate forest lost	Veblen and Ashton (1978)
1970	Papua Guinea (Adelbert Range)	Earthquake $M=7.9$	Vegetation stripped from circa 25% of the surface	Pain and Bowler (1973), Schuster and Highland (2003)
1976	Panama (Southeast coast)	Earthquake $M=6.7$ and 7.0	Removal of about 54 km^2 of jungle	Garwood et al. (1979), Schuster and Highland (2003)
1982	USA	Mount St. Helens eruption and landslide	550 km^2 of forest lost	Collins and Dunne (1988)
1987	Ecuador	Reventador earthquakes $M=6.1$ and 6.9	More than 75% of the rainforest of the southwestern slopes of Reventador volcano and 230 km^2 of natural forest lost	Nieto et al. (1991), Schuster et al. (1996), Figueroa et al. (1987), Schuster and Highland (2003)
1994	Colombia	Paez earthquake $M=6.4$	250 km^2 of second-growth sub-tropical brush and forest lost	Martinez et al. (1995), Schuster and Highland (2003)
1998	El Salvador	Hurricane Mitch (floods and landslides)	1000 km^2 of forest damaged in protected areas or in the process of protection, 18,000 ha of riverside forests very seriously damaged	ECLAC (1999a)
1998	Guatemala	Hurricane Mitch (floods and landslides)	63 km^2 of riverside forest severely damaged	ECLAC (1999b)
1998	Honduras	Hurricane Mitch (floods and landslides)	10700 km^2 of protected areas, 150 km^2 riverside forest, 2034 km^2 managed forest, and 58 km^2 of the Guanaja Isle damaged	CEPAL (1999)
1998	Nicaragua	Hurricane Mitch (floods and landslides)	1917 km^2 of forest in protected areas or in the process of protection, and 51 km^2 of riverside forest damaged	ECLAC (1999c)
1999	Venezuela	Floods and landslides	33,503 ha of vegetation cover lost	CEPAL (2000)

northeastern sector of Puebla and is characterized by high levels of marginality. It is formed by the sierras of Chignahuapan, Huauchinango, Tetela de Ocampo, Teziutlan, Zacapoaxtla, and Zacatlan, with a maximum elevation of 4282 m asl. Intense erosion and gully development are common where landforms are structurally controlled by faults and fractures.

In October 1999 an extreme rainfall event was produced over the study area as a result of the interaction between a tropical depression and a cold front. The event triggered massive flooding and numerous landslides, significantly impacting human settlements and economic development. Mass movement processes included slides, flows, falls, and complex movements as a result of a combination of types. Such slope movements involved enormous volumes of material ranging from 10^2 to 10^6 m^3, producing landslide scars varying from 10 to 100 m, and in some cases up to several hundred meters. Landsliding took place particularly on the pyroclastic deposits widely extended in the studied area, in addition to Jurassic sedimentary rocks.

Data provided by the National Meteorological Service suggest that mean monthly precipitation values were exceeded within only a few days. In the town of Zacapoaxtla for instance, cumulative precipitation from October 3 to 6 reached 844 mm, the equivalent of 60% of the total average annual precipitation of 1421.2 mm. In Teziutlan village, 743 mm of precipitation fell during the same period, comparable to half of the total annual rainfall. In both cases the rain registered in October 5th was larger than the corresponding mean monthly values; in Zacapoaxtla it equaled 150%, while in Teziutlan 133% (Alcántara-Ayala, 2004). If antecedent rainfall over a longer time period is considered (Fig. 2), as well as the geological and geomorphic setting of the area, landsliding susceptibility can be easily regarded as a natural tangible landscape process. Moreover, coupling such factors as vulnerability of the areas because of the anthropogenic characteristics, risk levels increase drastically and result in disasters. Among the landsliding cases, the village of Teziutlan encountered tragic losses when 109 victims were claimed by la Aurora, a translational slide transformed into a mudflow on a slope formed by pyroclastic deposits. Other cases included Zacapoaxtla, a town established on gullies developed in pyroclastic materials overlaying basaltic lava flows. Building damage associated with slope movement stress remains a concern and is expressed through the formation of structural cracks.

Immediately after the event the regional Civil Protection Unit focused on assessing and characterizing the sites, as well as evaluating the areas having the highest level of risk (SEPROCI, 1999). The Civil Protection Unit identified 301 unstable landslide sites produced from the October 1999 rainfall event. All of these events were affecting local communities, rivers, dams, and roads. The total volume of material was calculated as 750,000,000 m^3 of unstable material. Most landsliding adjacent to populated areas occurred on pyroclastic deposits because of low shear strength and high levels of erosion. Such incidences

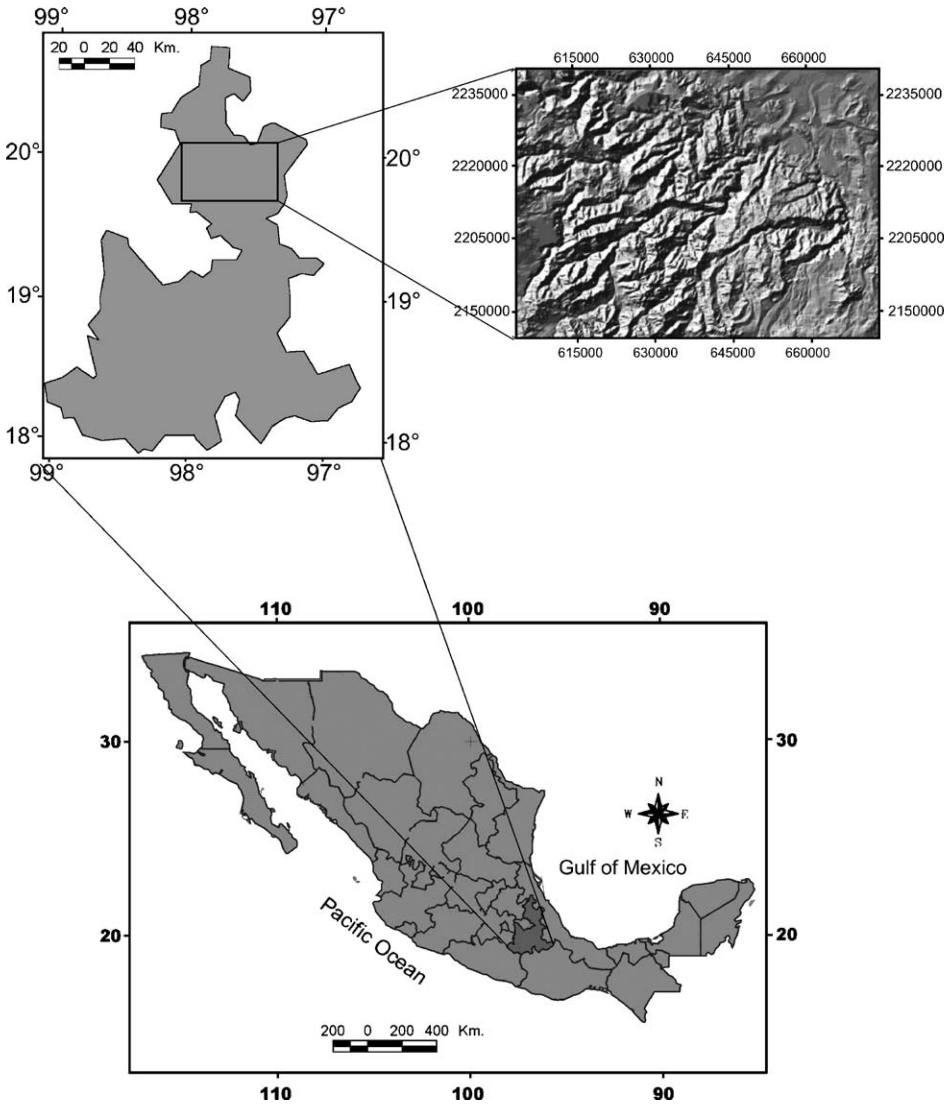

Fig. 1. Location of the Sierra Norte, Puebla.

accounted for 82% of the total evaluated unstable mass, whereas the corresponding 18% occurred on interbedded lutites and sandstones.

As a result of the Civil Protection Unit assessing the highest risk areas, 4715 people were subsequently relocated because they were on active mass failures or on zones prone

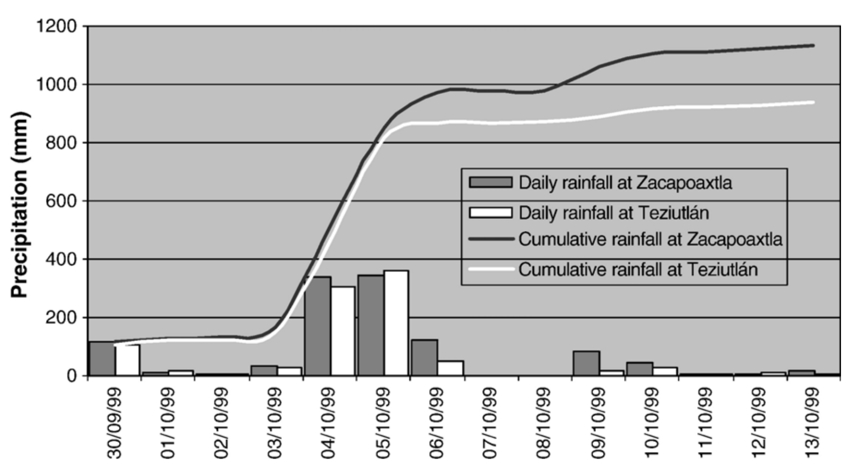

Fig. 2. Daily and cumulative rainfall that occurred in the Sierra Norte from September 30 to October 14, 1999.

Fig. 3. Landslide in the Zempoala River, October 1999.

to flooding. Evaluations were also undertaken along the Apulco and Zempoala Rivers. On the former, 10,000,000 m^3 of material were involved on a landslide which could have triggered a movement of an additional volume of 20,000,000 m^3 and obstruction of the river, which is known to trigger flooding. Likewise, on the Zempoala River, at the north of the Zapotitlan village, a landslide comprising 48,000,000 m^3 of pyroclastic deposits affected the main roads and formed a dam (Fig. 3).

The consequences of this enormous natural disaster were 263 victims, and 1.5 million residents were affected, the equivalent of 30% of Puebla's population. Total damage was estimated at US$450 million (Bitrán and Reyes, 2000), and was concentrated on services and infrastructure (communications and transport), social (principally housing), and productive sectors (agriculture) (Table 4).

Table 4
Damage and consequences produced by flooding and landsliding in the Sierra Norte during October 1999 (Bitrán and Reyes, 2000)

Sectors	Millions of USD		
	Direct damage	Indirect damage	Total damage
Social sector	50.5	1.5	52
Housing	48.61	0	48.61
Education	1.64	1.5	3.14
Health	0.25	–	0.25
Services and infrastructure	154	0.1	154.1
Water	8.46	0.18	8.64
Energy	48.11	–	48.11
Communications and transport	97.43	–	97.43
Productive sector	19.07	3.5	22.57
Agriculture	13.25	3.5	16.7
Cattle	1.54	–	1.54
Forestal	3.5	–	3.5
Fishing	0.78	–	0.78
Total	447.14	10.28	457.37

2.2. Land use and vegetation cover in the Sierra Norte, Puebla

Deforestation, biodiversity, local and regional climate change, global warming, and land degradation and desertification are among the processes linked to land use change. According to studies that factor anthropogenic influence, global forests have decreased circa from one third to one half of their original cover (Noble and Dirzo, 1997; Cincotta et al., 2000), and is mainly associated with increasing population density (Cincotta et al., 2000). Estimates provided by FAO (1993) indicated a yearly tropical forest loss of 154,000 km^2 between 1980 and 1990, the equivalent of an annual mean deforestation rate of 0.8%. Particularly for Latin America, such estimates involved a decrease of 53% of the original forest and rainforest cover, having Brazil, Costa Rica, and Mexico as the main source of one third of the total estimate (FAO, 1996).

Attempts to assess forest losses in Mexico have provided variable estimates (Table 5), ranging from 365,000 (SARH, 1992) to 1,500,000 ha (Toledo, 1989). Such variance is due to the heterogeneity of approaches used, as well as a lack of

Table 5
Estimation of forest loss rates in Mexico

Source	Lost surface (ha/year)
SARH (1992)	365,000
SARH (1994)	370,000
Repetto (1988)	460,000
FAO (1997)	508,000
FAO (1998)	615,000
Masera et al. (1992)	668,000
FAO (1993)	678,000
Myers (1989)	700,000
Castillo et al. (1989)	746,000
Toledo (1989)	1,500,000

Table 6
Total and relative vegetation surface derived from the National Forest Inventory (source: Palacio et al., 2000; Mas et al., 2002; Velázquez et al., 2002)

Level 1	Level 2	Surface (ha)	%
Formations	Vegetation types and other land use coverages		
Cropland	Cropland (irrigation and humid)	45,687,017	23.53
	Cropland (annual basis)		
	Forest cropland		
Temperate forest	Conifers	32,850,691	16.92
	Conifers and broad-leaved		
	Broad-leaved		
	Mountain cloud forest		
Tropical forest	Perrenial and sub-perrenial rainforest	30,734,896	15.83
	Deciduous and sub-deciduous forests		
Scrubland	"Mezquital" xerophytic scrubland	55,451,788	28.55
Grassland	Grassland	18,847,355	9.71
Hygrophilous vegetation	Hygrophilous vegetation	2,082,584	1.07
Other vegetation types	Other vegetation types	6,198,623	3.19
	Apparently non-vegetated area		
Other coverage types	Human settlements	2,345,458	1.21
	Water reservoirs		
Total		194,198,411	100.00

adequate validation techniques. In order to improve certainty and database quality mechanisms a National Forest Inventory (NFI) of Mexico was recently developed (Palacio et al., 2000). According to the NFI, the current annual deforestation rate of temperate and tropical forests and scrubland for the whole country is 0.43%, involving a loss of circa 545,000 ha per year between 1976 and 2000. Such estimates coincide significantly with estimates from the Global Forest Resources Assessment 2000 (FAO, 2001). Table 6 shows total and relative vegetation surface derived from the NFI taking into account vegetation formations, vegetation types, and other land use coverages. Scrubland and cropland are the equivalent of 52% of the total cover, while temperate and rain forests cover 17% and 16% respectively.

The corresponding Sierra Norte sector was extracted from the NFI to correlate landslide spatial distribution and vegetation formations (Fig. 4). According to a general categorization (Table 7), grasslands and tropical forest occupy the biggest extension, with 38% and 33% respectively, whereas temperate forest and cropland cover 19% and 6% of the total area. Circa 50% of the registered landslides took place on cropland, followed by temperate forest (33%) and grassland (10%), while the corresponding 7% occurred on tropical forest and human settlements.

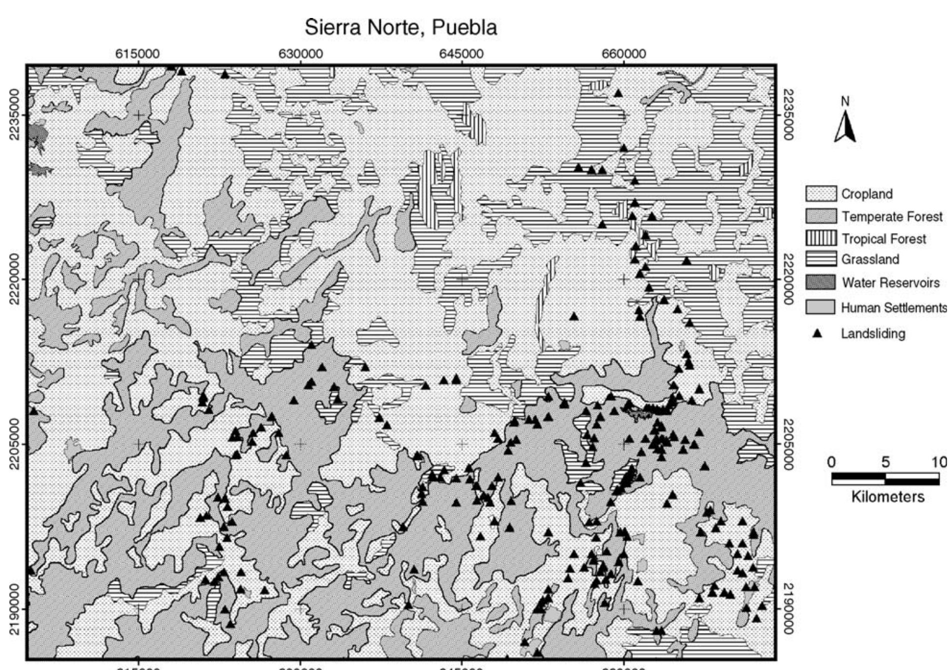

Fig. 4. Landslides distribution as a function of vegetation formations derived from the NFI.

Table 7
Types of vegetation cover derived from the NFI 2000 and landslides distribution in the studied area

Land use	Surface (km^2)	Number of landslides	Landslides (%)
Cropland	1213.51	145	49.15
Urban areas	12.57	15	5.08
Temperate forest	1179.52	98	33.22
Grassland	674.55	29	9.83
Tropical forest	37.04	8	2.72
Total		295	100

The NFI provided a general view of the land use of the Sierra Norte. However, since the accuracy cannot be extrapolated to a regional level because of the original scale of analysis, vegetation change was analyzed within the research area by using a remote sensing approach. This method was undertaken to more precisely characterize the pattern of landslide distribution in relation to vegetation conditions within the highly humanly transformed and disturbed area. No adequate imagery were available between 1989 and the October 1999 event. Nevertheless, the extensive database provided by the Civil Protection Unit of Puebla in response to the landslide disaster, and analysis of several aerial photographs, provided sufficient evidence to demonstrate that the October 1999 precipitation event was the triggering mechanism for the numerous mass movements.

3. Methods

3.1. Analytical procedure

Several algorithms have been proposed to undertake multi-temporal image analyses. These comprise various techniques, such as image differencing (Jensen, 1996; Singh, 1986; Fung and LeDrew, 1988; Coppin and Bauer, 1996), ratio of spectral bands, principal component analysis (Byrne et al., 1980; Fung and LeDrew, 1988; Coppin and Bauer, 1996), differentiation of vegetation indices (Tucker, 1979; Sellers, 1985; Singh, 1986; Lyon et al., 1998), regressions and linear transformations usually derived from thresholding, supervised or unsupervised spatial classification (Dymond and Shepherd, 2004), or temporal analysis (Lunetta et al., 2004). Such techniques have been satisfactorily used to monitor forest clearing as well as patterns and rates of land use change in diverse climatic and physical settings across the earth (FAO, 1993, 1996, 1997, 2001).

The main goal of this research was to analyze the spatial relationship of vegetation cover and rainfall induced landsliding by means of evaluating the land use changes occurred between 1989 and 1999. Therefore, satellite imagery was analyzed in terms of dynamic rescaling, NDVI, thresholding, and homogeneity. Satellite images comprised two images; a Landsat Thematic Mapper (TM) scene taken in October 1989, in addition to an ETM+ image recorded also in October 1999, but 2 weeks after the landsliding episode. Additionally, other Landsat satellite images dated August 1999 and 2000 were insufficient for analysis because of a high level of cloud cover.

3.2. Normalized vegetation index (NDVI) calculation

The normalized difference vegetation index (NDVI) involves a non-linear transformation of the visible or red and near-infrared bands of satellite images (Rouse et al., 1973; Jackson et al., 1983; Tucker et al., 1991), consequently NDVI results from the difference between the visible or red (RED, 0.58–0.68 μm) and near-infrared (NIR, 0725–1.1 μm) bands, and can be considered a measure of vegetation in terms of biomass, leaf area index, and percentage of vegetation cover. NDVI values range from −1 to +1 (pixel values 0–255) and is represented by Eq. (1).

$$\mathrm{NDVI}_{(i,j)} = \frac{\mathrm{NIR}_{(i,j)} - \mathrm{RED}_{(i,j)}}{\mathrm{NIR}_{(i,j)} + \mathrm{RED}_{(i,j)}} \tag{1}$$

where: (i, j) are coordinates of points.

Vegetation indices derived from satellite images have been extensively utilized to monitor vegetation and land use changes, particularly NDVI. This index is a function of red and near-infrared spectral bands which depends on the type of sensor. Therefore, when images from different sensors are analyzed, variations resulted from the images spectral, spatial and radiometric resolution characteristics need to be cross-calibrated; after such treatment comparison of images can be undertaken.

3.3. Dynamic rescaling

As a first stage to produce comparable results and to follow up the vegetal cover evolution in a more accurate way, the two images were treated by using an adaptive stretching of the main lines. Each scene was scanned following the raw order and then summed inside a 3×3 sliding window considering the values of the studied pixel and of its neighbors. Pixels of vicinity 4 were used. When the whole scene was scanned, the minimum (m) and the maximum (M) values obtained allowed replacing the dynamic scale in the range (0, 255).

$$P_{(i,j)} = \left[\left(V_{(i,j)} - m\right)/(M - m)\right] \times 255 \tag{2}$$

where i and j are the coordinates of the pixel P, and V is the result of the summation formerly described.

In order to avoid any aliasing resulting from stretching, the V value corresponded to a float number. Afterwards P was normalized between 0 and 255.

3.4. Thresholding

After normalizing the NDVI index between −1 and 1, it was possible to define the value of the point 0 in the rescaled image in order to emphasize the local variation of the vegetal cover. For instance, considering that the NDVI was normalized (0, 255), if the threshold retained was higher than 128, the lower saturation blurred the values that did not correspond to the vegetation; therefore dynamic scale of vegetation was stretched. Subsequently, there was a possibility to either apply a supervised threshold by using the results of the national forest inventory, or to apply an automatic treatment, such as equi-population segmentation, or considering values derived from rescaled histograms. As we did rescaling, we considered the median (maximum point of the histogram, higher than 128) in order to define the threshold value. Resulting images were presented in binary form. Such an approach allowed comparing results of both data sets.

3.5. Homogeneity

Research concerning landscape fragmentation has included land cover classifications as well as comparisons with vegetation indices (Southworth et al., 2004). It involves the homogeneity notion as an important feature that indicates the degree of fragmentation of the studied item, in this case, vegetation. The process involves considering a quadratic sliding window, where number of pixels with the same value as the central pixel are summed. In this case, as the threshold image is a binary image, the code 1 is searched. This sum is divided by the total number of pixels forming the sliding window, i.e. in a 3×3 sliding window this number is equal to 9. Therefore, the homogeneity percentage ϖ of the studied pixel is equal to:

$$_{(i,j)} = \sum_{l=1}^{l=n^2} Pbi(l)/n^2 \quad (3)$$

where i and j are the coordinates of the studied pixel, Pbi the pixels inside the sliding window, which have the same value as the value of the central pixel, and n the size of the sliding window side.

The involved treatment consisted of applying the above-mentioned procedure using sliding windows of increasing size (3, 5, 7, 9 and 11) and then counting according to a given threshold of homogeneity (i.e., 75%) the total number of pixels extracted by using this threshold on each sliding window size. According to such procedure and taking into account resolution of available data, it was possible to determine that the size of the window side of 11 was the most appropriated to study fragmentation in this region.

Even if forest degradation and land-cover change seems to play an important role in mass movement, our purpose in this paper did not involve only studying vegetation fragmentation (Fig. 5), it also concerned the relation between changes on land-cover and landsliding occurrence and distribution. With such a goal, all the points that correspond to the localization of the landslides observed in the studied region were reported in an image in order to

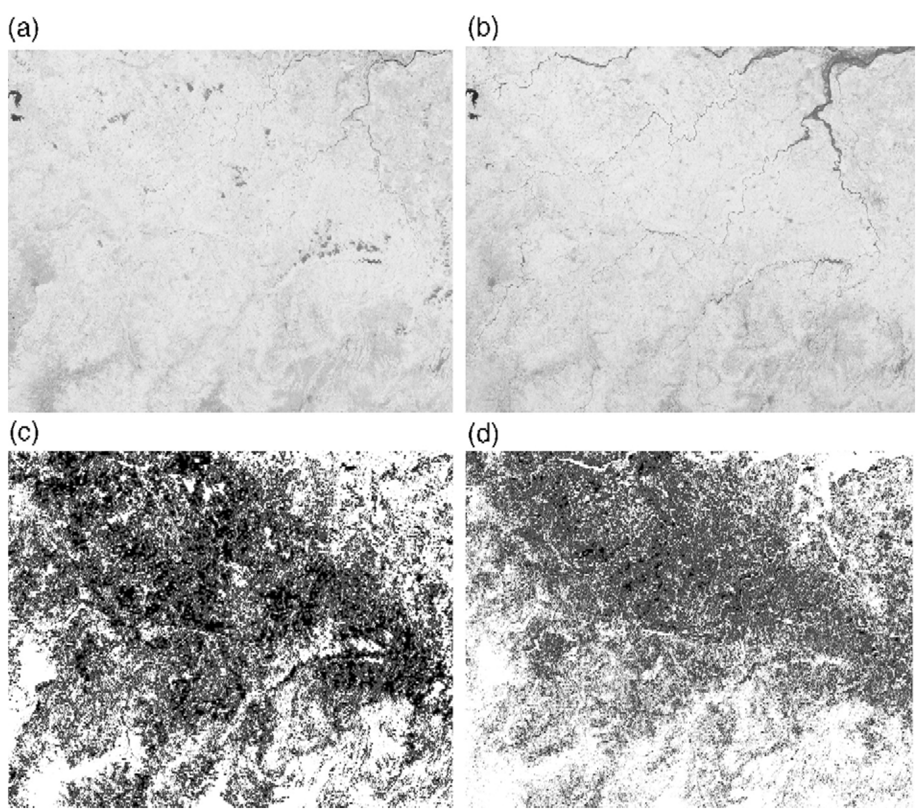

Fig. 5. NDVI indexes and vegetation density derived from homogeneity using an 11×11 moving window. Black colors indicate 100% of vegetation density, and gray tones means decreasing density. (a) NDVI 1989, (b) NDVI 1999, (c) density of vegetation 1989, (d) density of vegetation 1999.

establish the correlation existing between these locations and the nature of the vegetal cover.

3.6. Spatial representation of fragmentation

In order to define and analyze the spatial patterns of the vegetal cover fragmentation from 1989 to 1999, we used the two binary images that were formerly utilized to calculate homogeneity. All fragments of the size comprised between 1 and 5 ha (that is to say in this case between 11 and 55 pixels) were extracted. Total number of pixels which corresponded to those fragments was equal to 270, 270 and 707, 758 in 1989 and 1999 respectively, showing that this phenomenon increased strongly comparing these two dates.

The second step concerned the definition of the zones that were characterized by a fragmentation process. The procedure consisted of scanning the image by means of a moving circle with the idea of emphasizing the spatial representation of fragmentation by using a radius equal to 50 pixels, that is to say 1500 m. On each position (i, j) of the circle center, the total number of binary pixels corresponding to the different connected components covered by the circle were summed. This sum was reported at the position (i, j).

Fig. 6 shows the extent of the fragmented zones in 1989 and 1999, as well as the crossing of the two areas. The fragmented zones of 1989 are represented with a clear gray tone, the fragmented zones of 1999 in darkest, and the intersection with dark gray. The extension of the vegetation fragmentation followed a pattern from the periphery to the central area. During 1989, dense vegetation cover as well as high level of fragmentation can be observed in the border of the active vegetation zone. On the other hand, in 1999 fragmentation occurred where fragmentation had previously occurred (dark gray tone of Fig. 6) and additionally it continues growing towards the center (darkest tone). It is worthwhile to mention that the figure for 1999 clearly expresses the level of fragmentation or state of vegetation at the time of the landslide occurrence.

4. Results and discussion

Statistical distribution of vegetation concentration levels coupled with the spatial incidence of landsliding enabled a diachronic analysis of hillslope instability distribution in the Sierra Norte, Puebla, Mexico. Results indicate a significant fragmentation, and hence vegetation reduction from 1989 to 1999 (Fig. 7). Bare surfaces, represented by 0% of vegetation density, increased from 2688 km^2 in 1989 to 3496 km^2 in 1999. In general there was a tendency to have areas with lower values of vegetation density. For instance, in 1989 a surface of 336 km^2 comprised a density of vegetation between 1% and 50%, whereas 10 years later the area was as high as 553 km^2. Additionally, considering zones of higher vegetation, particularly with density between 50% and 100%, there was a strong decrease, 60% of vegetation was affected and the area diminished from 2582 to 1555 km^2. If all vegetation areas (from 1% to 100% of density) are taken into account, a decade of land use change clearly illustrated different levels of fragmenta-

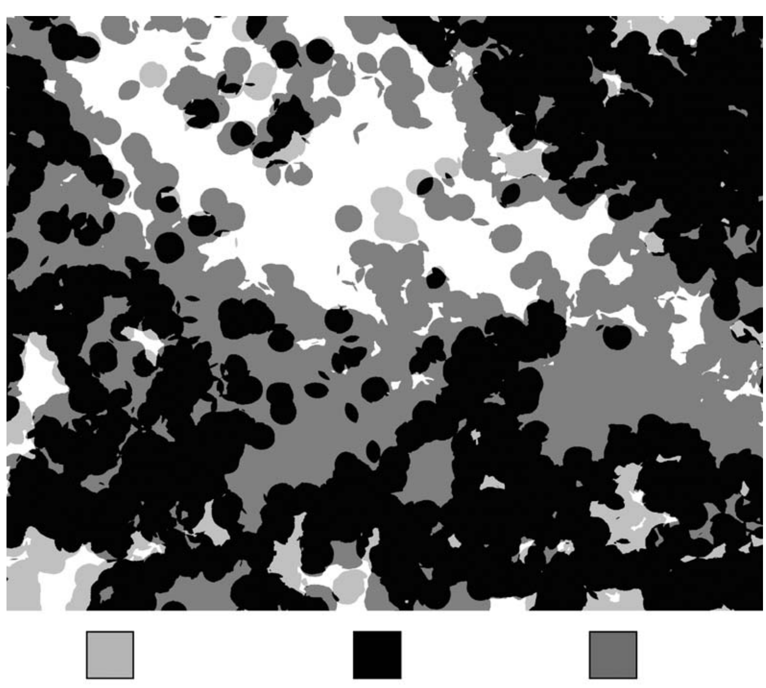

Fig. 6. Representation of vegetation fragmentation.

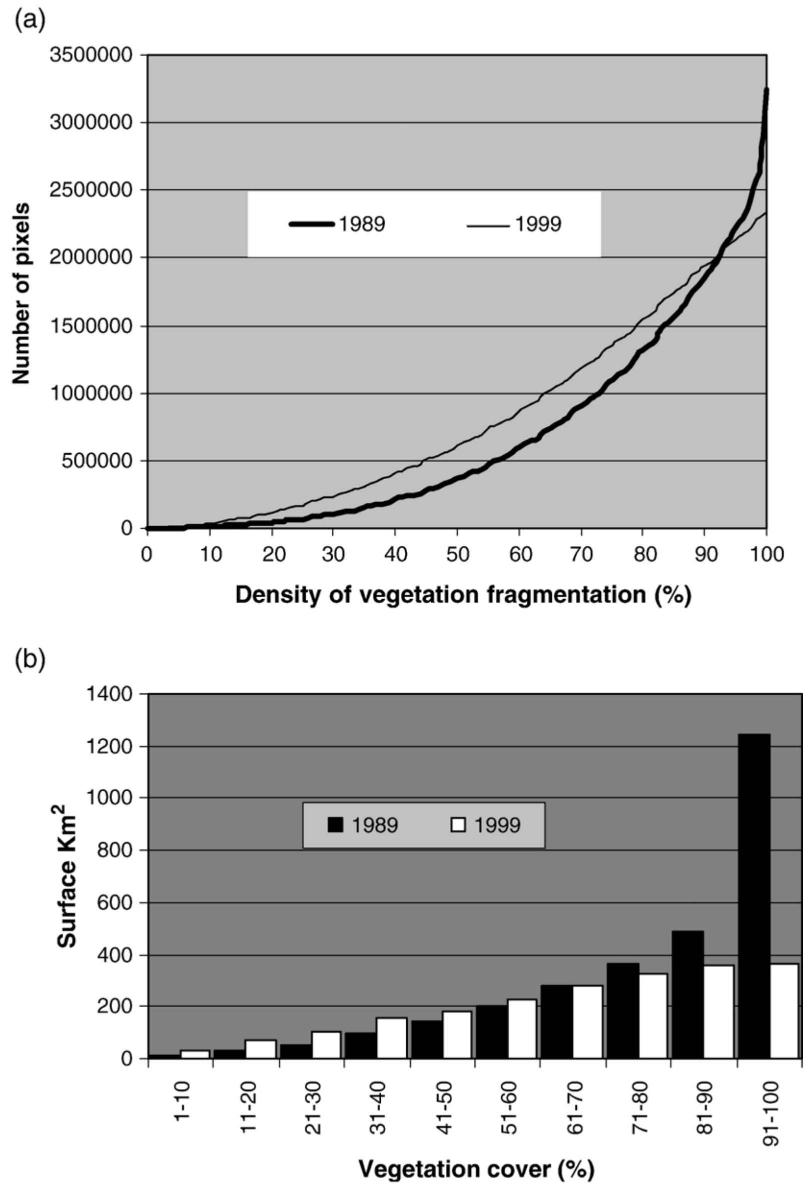

Fig. 7. (a) Vegetation density cumulative histogram (number of pixels per image). (b) Percentage of vegetation density ranges.

tion, which as a whole reveals that the area of vegetation decrease was 809 km^2. Moreover, there was a considerable reduction of vegetation areas ranging between 91% and 100% of density, whereas in 1989 it counted for 1245 km^2, 70% of the cover disappeared decreasing up to an area of 363 km^2 (Table 8).

From the 301 landslides points identified by the Puebla Civil Protection Unit (SEPROCI, 1999), 295 occurred within the research area. To analyze the correlation between the distribution of slope instability and the spatial pattern of vegetation cover, the location of registered landslides was combined with the vegetation fragmentation produced for 1999. According to the incidence of landsliding on the different vegetation cover ranges, 250 landslides, corresponding to 85% of the total mass failures, occurred on areas where the density of vegetation ranged between 0% and 50%, which represent bare soils and poorly vegetated areas. Distinctively, 72% of the landslides occurred on zones with the lowest values of vegetation density ranging from 0% to 10%, whereas 45 landslides where distributed on areas with vegetation covers with densities between 51% and 100% (Fig. 8).

From a global perspective deforestation is associated with a diverse array of environmental change, and within developing countries it is one of the major issues linked to natural hazards. Mexico has been affected by the consequences of land use change, which may have societal implications because of increasing frequency of disasters. The impact of land use change on hazards such as landsliding is of major interest for disaster prevention. In particular, for areas affected by strong seasonal precipitation or extreme meteorological events, the assessment of

Table 8
Vegetation changes resulted from the multi-temporal imagery analysis

Vegetation density (%)	Image of 1989		Image of 1999		
	Surface (km^2)	Surface (%)	Surface (km^2)	Surface (%)	Landslides (%)
0–10	2697.8	48.1	3529.5	62.9	71.8
11–20	29.3	0.52	71.3	1.2	1.3
21–30	54.2	0.96	107.3	1.9	4.4
31–40	99.3	1.78	157.4	2.8	2.3
41–50	142.7	2.5	183.7	3.2	4.7
51–60	204.2	3.6	230.3	4.1	4.0
61–70	277.3	4.9	280.6	5.0	2.7
71–80	364.2	6.5	326.2	5.8	3.3
81–90	490.6	8.7	355.6	6.3	3.0
91–100	1245.1	22.2	362.7	6.4	2.0
Total	5604.96	100	5604.96	100	100

landslide potential is essential. For the case of the Sierra Norte, the impact of forest clearance on mass movements was illustrated by analyzing vegetation density changes, in addition to the association of landslide distribution to land use according to the National Forestry Inventory of Mexico, which indicated that 52% of the vegetation coverage, without considering bare surfaces, has been subjected to human influence.

The significant role played by land-cover change, to a great extent represented by bare surfaces, on the incidence of landsliding suggests that the order of cause and effect between land-cover change (vegetation change) and landslides should be considered. In the case of the Sierra Norte it is implied that landsliding is a consequence of the reduction in the density of vegetation, which in many instances resulted in bare surfaces. Alternatively, it should be noted that other studies have found (see review by Blaschke et al., 2000) that landsliding is the driver of a reduction in vegetation, largely associated with a removal of organic matter and nutrients. However, while this may be the case of some sites reported by other researchers, it was clearly not the case for the data analyzed in this study. Indeed, the authors' (unpublished data) field observations noted vegetation growth at a number of the 1999 landslide sites 5 years after the event. All the same, it was demonstrated that for the decade analyzed, areas lacking vegetation resulted from land-cover change were more susceptible to hillslope instability.

5. Conclusions

Data obtained from this preliminary investigation expressed the relationship between vegetation fragmentation and the distribution of landsliding within the Sierra Norte in Puebla, Mexico. Vegetation cover was considered in terms of low (0–50%) and high (51–100%) vegetation density. Areas of high vegetation density were reduced considerably from 1989 to 1990, whereas the opposite situation occurred with low density areas. The former was associated with a decrease from 2581 km^2 to 1555 km^2 of vegetation over the 11 year study period, while the areas of low vegetation density increased from 336 km^2 to 553 km^2. In particular, should be those that underwent high or dense vegetation in 1989 to low vegetation density in 1999. Vegetation areas with the greatest density (91–100%) decreased dramatically from 1245 to 363 km^2, resulting in a net reduction in vegetation of 70%. Moreover, it was possible to highlight that landslide concentration was much higher on bare and low vegetation density areas (0–50%), representing 85% of hillslope instability, than on areas where vegetation cover had high density.

Results of this investigation support in two different ways the argument of the significant role of forest clearance induced by land-cover change on the occurrence of landsliding. First, based on the National Forest Inventory, 50% of the landslides were distributed on areas with no natural vegetation cover. Secondly, and the most important

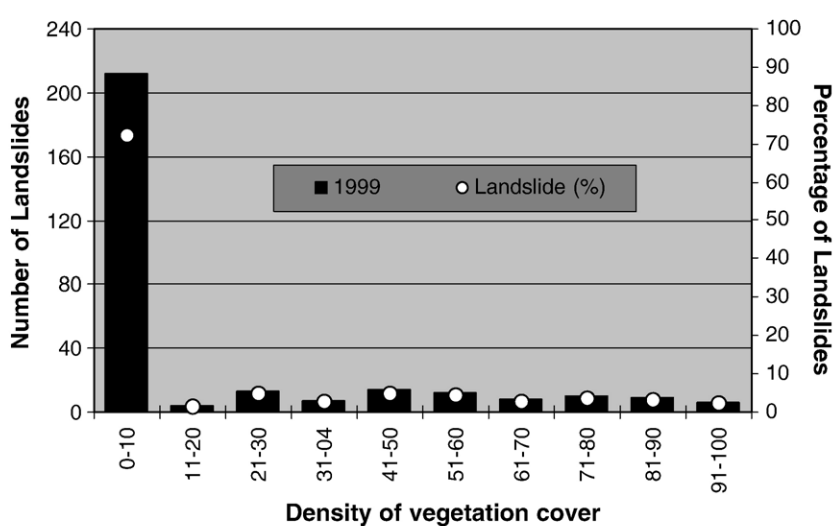

Fig. 8. Vegetation density percentage in relation to landsliding occurrence in 1999.

point, according to the remote sensing analysis of satellite images, the major incidence of landslides occurred on areas that underwent the greatest reduction in vegetation density between 1989 and 1999. Surfaces having less than 50% of vegetation cover were particularly susceptible to landslides. Land-cover change that resulted in low vegetation densities and bare surfaces between 1989 and 1999 were the main sources of hillslope instability.

While the approach used by this study has offered a regional scale analysis of land use factors associated with landsliding and disasters, at a local scale it is important to undertake additional detailed studies to understand soil, vegetation, and geomorphic controls. For example, it would be useful to examine the vegetation from the standpoint of root strength, and the distribution of soil hydrology under varying combinations of topographic segments and lithology. Such studies are ongoing by the authors, and involve experimental plots representing different combinations of land use, vegetation, topography, and geology. Understanding these factors would provide added insight into the controls on landsliding when different types of land use change occur, and provide the opportunity to scale-up to regional level analysis using the approach adapted by this study. Understanding the impact of vegetation change to soil hydrology and consequently for distinct landslide mechanisms is an essential step in assessing the linkage between land degradation and landslide driven natural disasters, an issue of great relevance to tropical countries such as Mexico.

Acknowledgements

This research was undertaken as part of the Project J-33428-T kindly supported by CONACyT, and the assistance provided by DGAPA-UNAM through the PAPIIT Project IN310002-3. Thanks are also due to The OFDA/CRED International Disaster Database, Université Catholique de Louvain, Brussels, Belgium, for providing natural disasters data. Last but not least, we would like to acknowledge the anonymous referees for providing valuable comments and suggestions for the preparation of the final version of this paper.

References

Abe, K., Ziemer, R.R., 1991a. Effect of tree roots on a shear zone: modeling reinforced shear stress. Canadian Journal Forest Research 21 (7), 1012–1019.

Abe, K., Ziemer, R.R., 1991b. Effect of tree roots on shallow-seated landslides. Proceedings, Geomorphic Hazards in Managed Forests, XIV IUFRO World Congress, 5–11 August 1990, Montreal, Canada, USDA Forest Service Gen. Tech. Report PSW-130, Berkeley, California, pp. 11–20.

Alcántara-Ayala, I., 2002. Geomorphology, natural hazards, vulnerability and prevention of natural disasters in developing countries. Geomorphology 47, 107–124.

Alcántara-Ayala, I., 2004. Hazard assessment of rainfall induced landsliding in Mexico. Geomorphology 61, 19–40.

Alva-Valdivia, L.M., Goguitchaichvili, A., Urrutia-Fucugauchi, J., Ferrari, L., Rosas-Elguera, J., Zamorano-Orozco, J.J., 2000. Paleomagnetic data from the Trans-Mexican volcanic belt: implications for tectonics and volcanic stratigraphy. Earth, Planets and Space 52 (7), 467–478.

Bitrán, D., Reyes, C., 2000. Evaluación del impacto económico de las inundaciones ocurridas en octubre de 1999 en el estado de Puebla. In: Bitrán, D. (Ed.), Evaluación del impacto socioeconómico de los principales desastres naturales ocurridos en la República Mexicana durante 1999, Cuadernos de Investigación 50. CENAPRED, pp. 161–194.

Blaschke, P.M., Trustrum, N.A., Hicks, D.L., 2000. Impacts of mass movement erosion on land productivity: a review. Progress in Physical Geography 24 (1), 21–52.

Byrne, G.F., Crapper, P.F., Mayo, K.K., 1980. Monitoring land cover change by principal components analysis of multi-temporal Landsat data. Remote Sensing of Environment 10, 175–184.

Castillo, P.E., Lehtonen, P., Simula, M., V. Sosa, R., 1989. Proyecciones de los principales indicadores forestales de México a largo plazo (1988–2012). Reporte interno, Subsecretaría Forestal, Cooperación México-Finlandia. SARH, México.

CEPAL, 1999. Honduras: evaluación de los daños ocasionados por el Huracán Mitch, 1998. Sus implicaciones para el desarrollo económico y social y el medio ambiente.

CEPAL, 2000. Los efectos socioeconómicos de las inundaciones y deslizamientos en Venezuela en 1999: Perfiles de proyectos.

Cincotta, R.P., Winsnewski, J., Engelman, R., 2000. Human population in the biodiversity hotspots. Nature 404, 990–991.

Collins, B.D., Dunne, T., 1988. Effects of forest land management on erosion and revegetation after the eruption of Mount St. Helens. Earth Surface Processes and Landforms 13 (3), 193–205.

Coppin, P.R., Bauer, M.E., 1996. Digital change detection in forest ecosystems with remote sensing imagery. Remote Sensing Reviews 13, 207–234.

De La Ville, N., Diaz, A.C., Ramirez, D., 2002. Remote sensing and GIS technologies as tools to support sustainable management of areas devastated by landslides environment. Development and Sustainability 4 (2), 221–229.

Dymond, J.R., Shepherd, J.D., 2004. The spatial distribution of indigenous forest and its composition in the Wellington region, New Zealand, from ETM+ satellite imagery. Remote Sensing of Environment 90 (1), 116–125.

ECLAC, 1999a. El Salvador: assessment of the damage caused by hurricane Mitch, 1998. Implications for Economic and Social Development and for the Environment.

ECLAC, 1999b. Guatemala: assessment of the damage caused by hurricane Mitch, 1998. Implications for Economic and Social Development and for the Environment.

ECLAC, 1999c. Nicaragua: assessment of the damage caused by hurricane Mitch, 1998. Implications for Economic and Social Development and for the Environment.

EM-DAT: The OFDA/CRED International Disaster Database, Université Catholique de Louvain, Brussels, Belgium, http://www.em-dat.net/.

FAO, 1993. Forest resources assessment 1990: tropical countries. Forestry Paper 112 (Rome).

FAO, 1996. Forest resources assessment 1990. Survey of tropical forest cover and study of change processes. Forestry Paper 130 (Rome).

FAO, 1997. State of the World Forest in 1997. FAO, Roma.

FAO, 1998. An Intern Report on the State of Forest Resources in the Developing Countries, Forest Resource Division. Forestry Department, Roma.

FAO, 2001. Global forest resources assessment 2000. FAO Forestry Paper 140 (Rome).

Figueroa, E., Oviedo, G., Vela, C., et al., 1987. Evaluación del Impacto Ambiental del Ssimo en la Amazonîa. Fundación Natura, Quito.

Fung, T., LeDrew, E., 1988. The determination of optimal threshold levels for change detection using various accuracy indices. Photogrammetric Engineering and Remote Sensing 54, 1449–1454.

Garwood, N.C., Janos, D.P., Brokaw, N., 1979. Earthquake-induced landslides: a major disturbance to tropical soils. Science 205, 997–999.

Gerrard, J., Gardner, R., 2002. Relationships between landsliding and land use in the Likhu Khola drainage basin, Middle Hills, Nepal. Mountain Research and Development 22 (1), 48–55.

Glade, T., 2003. Landslide occurrence as a response to land use change: a review of evidence from New Zealand. Catena 51 (3–4), 297–314.

Jackson, R.D., Slater, P.N., Pinter, P.J., 1983. Discrimination of growth and water stress in wheat by various vegetation indices through clear and turbid atmospheres. Remote Sensing of the Environment 15, 187–208.

Jensen, J.R., 1996. Introductory Digital Image Processing: A Remote Sensing Perspective, Upper Saddle River, 2nd ed. Prentice Hall, NJ. 316 pp.

Keppeler, E.T., Ziemer, R.R., Cafferata, P.H., 1994. Changes in soil moisture and pore pressure after harvesting a forested hillslope in northern California, 205–214. In: Marston, Richard A., Hasfurther, Victor R. (Eds.), Proceedings, Annual Summer Symposium of the American Water Resources Association: Effects of Human-Induced Changes on Hydrologic Systems, Jackson Hole, Wyoming. American Water Resources Association, Bethesda, Maryland.

Lunetta, R.S., Johnson, D.M., Lyon, J.G., Crotwell, J., 2004. Impacts of imagery temporal frequency on land-cover change detection monitoring. Remote Sensing of Environment 89 (4), 444–454.

Lyon, J.G., Yuan, D., Lunetta, R.S., Elvidge, C.D., 1998. A change detection experiment using vegetation indices. Photogrammetric Engineering and Remote Sensing 64, 143–150.

Marshall, A.J., 1937. Northern New Guinea, 1936. Geographical Journal 89 (6), 489–506.

Marston, R.A., Miller, M.M., Devkota, L.P., 1998. Geoecology and mass movement in the Manaslu-Ganesh and Langtang-Jugal Himals, Nepal. Geomorphology 26 (1–3), 139–150.

Martinez, J., Avila, G., Agudelo, A., Schuster, R.L., Casadevall, T.J., Scott, K.M., 1995. Landslides and debris flows triggered by the 6 June 1994 Paez earthquake, southwestern Colombia, Landslide News. Japan Landslide Soc. vol. 9, pp. 13–15.

Mas, J.-F., Peralta, A., Prado, J., Velázquez, A., Palacio-Prieto, J.L., Bocco, G., 2002. Assessing forest resources in Mexico: wall-to-wall land use/cover mapping. Photogrammetric Engineering and Remote Sensing 68 (10), 966–968.

Masera, O., Ordóñez, M.J., Dirzo, R., 1992. Emisiones de carbono a partir de la deforestación en México. Ciencia 43, 151–153.

Montgomery, D.R., Schmidt, K.M., Greenberg, H., Dietrich, W.E., 2000. Forest clearing and regional landsliding. Geology 28, 311–314.

Myers, N., 1989. Deforestation Rates in Tropical Forest and their Climatic Implications. Friends of the Earth, London.

Nieto, A.S., Schuster, R.L., Plaza-Nieto, G., 1991. Mass wasting and flooding. In: Schuster, R.L. (Ed.), The March 5, 1987, Ecuador Earthquakes—Mass Wasting and Socioeconomic Effects, Natural Disaster Studies, Natural Res. Council, Wash., D.C. vol. 5, pp. 51–82.

Noble, I.R., Dirzo, R., 1997. Forest as human dominated ecosystem. Science 277, 522–525.

Pain, C.F., Bowler, J.M., 1973. Denudation following the November 1970 earthquake at Madang, Papua New Guinea. Zeitschrift für Geomorphologie. Supplementband 18, 92–104.

Palacio, J.L., Bocco, G., Velásquez, A., et al., 2000. La condición actual de los recursos forestales en México: resultados del inventario forestal nacional 2000. Investigaciones Geográficas, UNAM, Boletín del Instituto de Geografía núm vol. 43, pp. 183–203.

Pande, A., Joshi, R.C., Jalal, D.S., 2002. Selected landslide types in the Central Himalaya: their relation to geological structure and anthropogenic activities. Environmentalist 22 (3), 269–287.

Repetto, R., 1988. The Forest for the Trees? Government Policies and the Misuse of Forest Resources. World Resource Institute, Washington, DC.

Rouse Jr., J.W., Haas, R.H., Schell, J.A., Deering, D.W., 1973. Monitoring vegetation systems in the Great Plains with ERTS. Proc. Earth Res. Tech. Satellite-1 Symp. Goddard Space Flight Cent., Washington, DC, pp. 309–317.

SARH, 1992. Inventario Forestal Nacional de Gran Visión. Reporte Principal. Secretaría de Agricultura y Recursos Hidráulicos, Subsecretaría Forestal y de Fauna Silvestre, México. 49 pp.

SARH, 1994. Inventario Forestal Nacional Periódico, México 94. Memoria Nacional Secretaría de Agricultura y Recursos Hidráulicos, Subsecretaría Forestal y de Fauna Silvestre, México. 81 pp.

Schuster, R.L., Highland, L.M., 2003. Impact of landslides and innovative landslide-mitigation measures on the natural environment. Proceedings of the International Conference on Slope Engineering. University of Hong Kong, Hong Kong, China.

Schuster, R.L., Nieto, A.S., O'Rourke, T.D., Crespo, E., 1996. Mass wasting triggered by the 5 March 1987 Ecuador earthquakes. Engineering Geology 42, 1–23.

Sellers, P.J., 1985. Canopy reflectance, photosynthesis, and transpiration. International Journal of Remote Sensing 6, 1335–1372.

SEPROCI, 1999. Investigación de riesgo en taludes y laderas naturales de la Sierra Norte y Nororiental del estado de Puebla (unpublished report).

Simonett, D.S., 1967. Landslide distribution and earthquakes in the Bewani and Torricelli Mountains. In: Jennings, J.N., Mabbutt, J.A. (Eds.), Landform Studies from Australia and New Guinea. National Univ. Press, Canberra, pp. 64–84.

Singh, A., 1986. Change detection in the tropical forest environment of northeastern India using Landsat. In: Eden, M.J., Pary, J.T. (Eds.), Remote Sensing and Tropical Land Management. John Wiley and Son, Chichester, pp. 237–254.

Southworth, J., Munroe, D., Nagendra, H., 2004. Land cover change and landscape fragmentation—comparing the utility of continuous and discrete analyses for a western Honduras region agriculture. Ecosystems and Environment 101 (2–3), 185–205.

Su, W.J., Stohr, C., 2000. Aerial-photointerpretation of landslides along the Ohio and Mississippi rivers. Environmental and Engineering Geoscience 6 (4), 311–323.

Temesgen, B., Mohammed, M.U., Korme, T., 2001. Natural hazard assessment using GIS and remote sensing methods, with particular reference to the landslides in the Wondogenet area. Ethiopia Physics and Chemistry of the Earth, Part C: Solar, Terrestrial and Planetary Science 26 (9), 665–675.

Toledo, V.M., 1989. Bio-economic costs of transforming tropical forest to pastures in Latinoamérica. In: Hecht, S. (Ed.), Cattle Ranching and Tropical Deforestation in Latinoamerica. Westview Press, Boulder Colorado.

Tucker, C.J., 1979. Red and photographic infrared linear combinations for monitoring vegetation. Remote Sensing of the Environment 8, 127–150.

Tucker, C.J., Newcomb, W.W., Los, S.O., Prince, S.D., 1991. Mean and inter-year variation of growing-season normalized difference vegetation index for the Sahel 1981–1989. International Journal of Remote Sensing 12, 1113–1115.

Van Beek, L.P.H., Van Asch, Th.W.J., 2004. Regional assessment of the effects of land-use change on landslide hazard by means of physically based modelling. Natural Hazards 31 (1), 289–304.

Veblen, T.T., Ashton, D.H., 1978. Catastrophic influences on the vegetation of the Valdivian Andes, Chile. Vegetation 36 (3), 149–167.

Velázquez, A., Mas, J.F., Palacio-Prieto, J.L., Bocco, G., 2002. Land cover mapping to obtain a current profile of deforestation in Mexico. Unisylva vol. 210, 53. FAO, Rome, Italy. http://www.fao.org/docrep/005/y4001e/Y4001E06a.htm.

World Bank Group, 2002. A Revised Forest Strategy for the World Bank Group. http://lnweb18.worldbank.org/ESSD/essdext.nsf/14Doc

ByUnid/8A104BE462BA75A385256BD00077F0DD/$FILE/FSSPFinal1Nov02pp1to28.pdf.

Wu, K., Thornes, J.B., 1996. Landslides and stability in the Nepalese Middle Hills under seasonal and agricultural land-use change scenarios Advances in hillslope processes. British Geomorphological Research Group Symposia Series 12, 773–797.

Ziemer, R.R., 1991. An approach to evaluating the long-term effects of land use on landslides, erosion, and stream channels. Proceedings, Japan-U.S. Workshop on Snow Avalanche, Landslide, Debris Flow Prediction and Control. 30 Sept–5 Oct 1991. Tsukuba, Japan. Organizing Committee of the Japan-U.S. Workshop on Snow Avalanche, Landslide, Debris Flow Prediction and Control, Tsukuba, Japan, pp. 533–542.